

Effects of irradiance transition characteristics on the mismatch losses of different electrical PV array configurations

ISSN 1752-1416

Received on 15th June 2016

Revised 22nd September 2016

Accepted on 14th November 2016

doi: 10.1049/iet-rpg.2016.0590

www.ietdl.org

Kari Lappalainen¹ ✉, Seppo Valkealahti¹¹Department of Electrical Engineering, Tampere University of Technology, Tampere, Finland

✉ E-mail: kari.lappalainen@tut.fi

Abstract: Photovoltaic (PV) systems are prone to irradiance fluctuations caused by overpassing cloud shadows which can be very large and steep. Cloud shadows have an average diameter of almost 1 km meaning that even the largest PV power plants are widely affected by them. Fast irradiance transitions can lead to failures in maximum power point tracking and to mismatch power losses due to partial shading of the PV generator. In this study, the effects of irradiance transition characteristics: shading strength, duration and apparent speed and direction of movement on the mismatch losses of PV generators were studied by simulations using a mathematical model of irradiance transitions and an experimentally verified MATLAB Simulink model of a PV module. The studied electrical PV array configurations were series–parallel, total-cross-tied and multi-string. Furthermore, three different physical shapes of the configurations were studied. On the basis of the results, module strings of PV arrays should be placed perpendicularly to the dominant apparent direction of movement of shadow edges and the diameter of the strings should be minimised to decrease the mismatch losses. Another finding of practical importance was that there were only minor differences between the mismatch losses of different electrical PV array configurations.

1 Introduction

Photovoltaic (PV) systems are prone to irradiance fluctuations caused by overpassing cloud shadows which are the main cause of fluctuating PV power production. With high penetration of grid-connected PV generators output power fluctuations can lead to problems in power balancing and quality. It has been found in [1] that the average diameter of cloud shadows is around 800 m meaning that even the largest PV power plants are widely affected by them. Furthermore, overpassing cloud shadows cause partial shading. Partial shading is the main cause of mismatch losses of PV systems, which are the difference between the sum of the global maximum power point (MPP) powers of individual modules and the global MPP power of the PV system. Furthermore, partial shading can lead to failures in MPP tracking causing extra losses. Partial shading can be due to, inter alia, passing clouds, surrounding objects, snow or soiling.

The effects of partial shading on the operation of PV generators have been studied in several papers, e.g. [2–10]. The operation of several different PV array configurations has been studied in these papers, but the focus has typically been on static partial shading conditions. Operation of PV generators under partial shading conditions caused by moving clouds have been studied, e.g. in [11–14]. Behaviour of mismatch losses under partial shading caused by moving clouds has been studied earlier in [11, 12]. It has been noticed that the movement direction of shadows has a substantial effect on the mismatch losses. The mismatch losses of traditional series–parallel (SP), total-cross-tied (TCT) and multi-string (MS) electrical PV array configurations caused by a moving shadow are the smallest when the shadow edge moves perpendicular to the PV module strings. In [12], the effects of the sharpness of shadows, i.e. the length of irradiance transitions, on the mismatch losses of PV generators have been studied during irradiance transitions caused by moving clouds. It has been found that the sharpness has a considerable effect on the mismatch losses. However, a comprehensive research of the effects of irradiance transition characteristics on the mismatch losses has not been presented earlier.

The variability of solar radiation and irradiance transitions caused by edges of moving cloud shadows have been studied, e.g. in [15–21]. In [18], an extensive analysis and a mathematical model of irradiance transitions caused by overpassing cloud

shadows have been presented. It has been found that shading strength (SS) of irradiance transitions varies from very thin shadings up to 90% and irradiance can change over 300 W/m² in 0.1 s. Thus, irradiance transitions caused by overpassing cloud shadows can be very large and steep. The duration of irradiance transitions varies a lot from a second up to several minutes. In [1], a comprehensive analysis of shading periods caused by moving clouds has been presented. It has been found that the duration of shading periods varies from a few seconds up to almost 1.5 h and that the speed of shadows varies considerably with an average value of around 13 m/s. However, when a shadow is covering a PV array the apparent speed of the shadow edge, i.e. the speed perpendicular to the edge of the shadow, actually defines how fast the PV array is getting shaded. Thus, apparent velocity of a linear shadow edge is a vital quantity in analyses of the effects of overpassing cloud shadows on the operation of small PV systems and PV arrays of large PV power plants while the supposition of linearity for the cloud edge is not valid with large power plants as a whole [19]. In [19], a comprehensive study of apparent velocity of shadow edges caused by moving clouds has been presented, and it has been found that the average value of apparent shadow edge speed is around 9 m/s and that the length of irradiance transitions caused by edges of moving clouds is typically around 100 m.

This paper presents a study of the effects of irradiance transition characteristics: SS, duration and apparent speed and direction of movement on the mismatch losses of PV generators. The studied PV array configurations were SP, TCT and MS. Furthermore, three different physical shapes of the configurations were studied. The study was conducted by using the mathematical model of irradiance transitions [18] and an experimentally verified MATLAB Simulink model of a PV module based on the well-known one-diode model of a PV cell. The effects of the irradiance transition characteristics were studied one by one by changing the value of the studied variable while keeping the other variables fixed at their typical, experimentally observed values [22]. The main novelty of this work with regard to previous studies of mismatch losses under partial shading conditions caused by moving clouds, e.g. [11, 12], is the use of more realistic shading scenarios based on the observed values and on the mathematical model of irradiance transitions instead of assumptions and simplifications. Moreover, in this paper, the simulations were

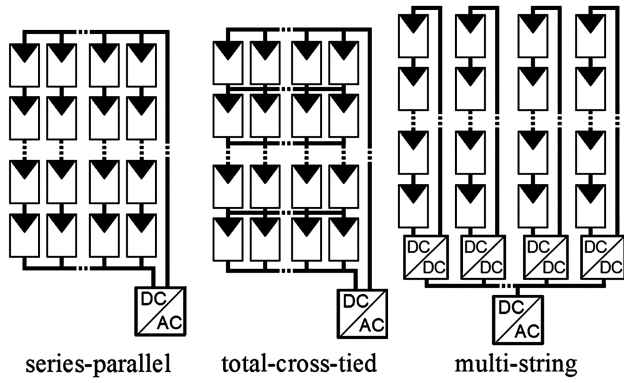


Fig. 1 Electrical connections of the studied PV array configurations

conducted by time steps of 0.1 s ensuring that even the fastest irradiance transitions phenomena were taken into account. The results of this work are relevant from electricity production point of view and also from output power fluctuations point of view since mismatch losses are the reason why the power of a PV array may change significantly faster than the average irradiance on the array [23].

2 Methods

2.1 Simulation model

The simulations were conducted by using an experimentally verified MATLAB Simulink model of a PV module based on the model presented by Villalva *et al.* [24]. The model is based on the well-known one-diode model which provides the following relation between the current and voltage of a PV cell:

$$I = I_{ph} - I_o \left(e^{\frac{(U + R_s I)}{A U_T}} - 1 \right) - \frac{U + R_s I}{R_{sh}}, \quad (1)$$

Table 1 Electrical characteristics of the NAPS NP190GKg PV modules in short-circuit (SC), open-circuit (OC) and MPP in STC

Parameter	Value
$I_{SC, STC}$	8.02 A
$U_{OC, STC}$	33.1 V
$P_{MPP, STC}$	190 W
$I_{MPP, STC}$	7.33 A
$U_{MPP, STC}$	25.9 V

Table 2 Constant parameter values of the simulation model for the NAPS NP190GKg PV modules and the bypass diodes

Parameter	Value
A	1.30
R_s	0.329 Ω
R_{sh}	188 Ω
A_{bypass}	1.50
$R_{s, bypass}$	0.020 Ω
$I_o, bypass$	3.20 μA

Table 3 Numbers of modules and the dimensions of the studied PV arrays

Number of modules (parallel x series)	Dimensions, m
6 x 28	14.2 x 41.3
8 x 21	19.6 x 31.0
12 x 14	30.4 x 20.7

where I is the current, I_{ph} is the light-generated current, I_o is the dark saturation current, U is the voltage, R_s is the series resistance, A is the ideality factor, U_T is the thermal voltage and R_{sh} is the shunt resistance of the PV cell [25]. Thermal voltage of a PV cell is defined by $U_T = kT/q$, where k is the Boltzmann constant, T is the temperature of the cell and q is the elementary charge. The simulation model of a PV module was obtained by scaling the parameter values used in the model of a PV cell by the number of PV cells in the PV module.

The characteristic of the simulation model was fitted to the electrical characteristics of the NAPS NP190GKg PV module, which are used in the solar PV power station research plant of Tampere University of Technology [26]. The module is composed of 54 series-connected polycrystalline silicon PV cells and three bypass diodes, each of them connected in anti-parallel with 18 cells. Electrical characteristics of the module given by the manufacturer in standard test conditions (STC) are presented in Table 1. Bypass diodes were modelled using (1) by assuming that the light-generated current I_{ph} is zero and the shunt resistance R_{sh} is infinite. The dark saturation current $I_o, bypass$, the series resistance $R_{s, bypass}$ and the ideality factor A_{bypass} of the bypass diodes were determined by means of curve fitting to a measured $I-U$ curve of a Schottky diode. The temperature of bypass diodes was assumed to be constant and the same as the module temperature. The simulation model parameter values for the modules and the bypass diodes are presented in Table 2.

The used simulation model is, naturally, a simplification of the reality containing simplifications and assumptions. However, the used simulation model enables fast computation and is accurate enough for the analysis presented in this paper. The experimental verification of the simulation model has been presented in detail in [5].

2.2 PV array configurations

In this paper, the mismatch losses of SP, TCT and MS PV array configurations were studied. The electrical connections of the studied configurations are presented in Fig. 1. SP and MS configurations are commonly applied in PV array installations, whereas TCT is frequently proposed in the literature for improving the PV generator performance [6, 7, 9, 11, 12]. In the configurations, series-connected PV modules are placed in straight strings of equal length forming a rectangle. There are no gaps between the series-connected modules and the distance between the strings is 2.0 m. The PV modules are mounted with a tilt angle of 45° from the horizontal plane. Three different lengths of series connections: 28, 21 and 14 modules were studied while the total number of modules was kept constant at 168. This array size was selected since it provides reasonable computing time, and since the string length of 28 modules is around the string length in typical PV arrays feeding inverters in utility scale PV power plants. Since PV arrays are the operational units of large PV power plants, the results achieved for these array sizes are largely valid for larger PV power plants. The nominal power of the studied generators under STC is 31.92 kWp. The studied arrays and their dimensions are presented in Table 3. The dimensions of the arrays were calculated by using the dimensions of the NAPS NP190GKg PV modules.

2.3 Shading of a PV array

Irradiance transitions caused by edges of overpassing cloud shadows were modelled by the mathematical model presented in [18]

$$G(t) = \frac{a}{1 + e^{\frac{(t-t_0)}{b}}} + c, \quad (2)$$

where G is the irradiance, t is the time, a is the change of irradiance and c is the minimum irradiance during the transition. Parameter b defines the duration of the transition and parameter t_0 adjusts the transition time defining the midpoint of the transition. The sign of parameter b defines whether the transition is a fall, i.e. a decreasing

irradiance transition or a rise, i.e. an increasing transition. In [18], the operation of the model has been validated with around 40,000 measured irradiance transitions and the average root-mean-square error of the curve fits to the measured transitions was around 12 W/m².

By utilising the mathematical model, irradiance transitions caused by shadows of moving clouds can be defined by four variables: SS, i.e. attenuation of irradiance due to shading, parameter b and apparent speed and direction of movement which have no correlation with each other [19, 22]. All the other variables needed to define irradiance transitions mathematically can be calculated from SS, b and initial irradiance. Parameters a and c were calculated from SS and initial irradiance. The duration of a transition was calculated by multiplying b with the experimentally obtained regression coefficient of 7.67 [22], and then parameter t_0 was calculated from the duration. SS of an irradiance transition, can be written as

$$SS = \frac{G_{us} - G_s}{G_{us}}, \quad (3)$$

where G_{us} is the irradiance of an unshaded situation and G_s is the irradiance under shading.

In this paper, PV systems with physical and electrical array layouts having two orthogonal lines of symmetry were studied. For these layouts, a situation of an overpassing irradiance fall is symmetrical to a situation of a similar overpassing irradiance rise. It has been found that the characteristics of irradiance falls and rises are in practice similar [18]. Thus, irradiance falls were used in the simulations to study the effects of irradiance transition characteristics. The symmetry of the array configurations also reduces the amount of studied apparent movement directions of shadow edges. When the layout has two orthogonal lines of symmetry, the amount of apparent movement directions reduces to 90°.

To simplify the computation, the temperature of PV modules was chosen to be the constant STC temperature of 25°C. During fast irradiance transitions, changes of module temperatures are small having only a negligible effect on the operation of the modules. Furthermore, it was chosen that before irradiance falls the PV array is under the constant STC irradiance of 1000 W/m².

The simulations were conducted by time steps of 0.1 s. A simulation period starts when a shadow edge moves over the first modules of the PV array and ends when the shadow edge has moved across the array, i.e. when all the modules are again uniformly shaded. The irradiance at the centre of each module with an accuracy of 0.1 W/m² was used as the irradiance of that module during a time step.

3 Results and discussion

The effects of SS, parameter b and apparent speed and direction of movement of irradiance transitions on mismatch losses were studied by changing the value of the studied variable while keeping the values of the other variables fixed. Typical shadow edge parameter values presented in Table 4 were applied as fixed values in the simulations. These values and the applied variable value ranges are based on experimentally observed values [18, 22]. By using these values, typical duration and length of irradiance transitions were 11.4 s and 89.2 m, respectively, and the length of a corresponding simulation period varied between 13 and 17 s depending on the dimensions of the array and the apparent movement direction of the shadow edge. The length of the simulation periods varied, respectively, from 2.5 to 99 s while

Table 4 Used fixed values of variables

Variable	Value
SS	57.8%
b	1.48 s
speed	7.86 m/s

changing the values of parameter b and apparent speed over their ranges.

The effects of SS, b and apparent speed on mismatch losses were studied with four apparent movement directions of shadow edges. The apparent movement directions are denoted with respect to series connections of the PV array, so that angle 0° denotes perpendicular and 90° parallel movement with respect to the series connections. The mismatch losses of a PV generator were calculated as the difference between the sum of the global MPP powers of the modules of the generator as if they were operating separately and the global MPP power of the generator. Relative mismatch losses were calculated with respect to the sum of the global MPP powers of the modules of the generator. The results of the studies of the effects of SS, parameter b and apparent speed and direction of movement are presented in Sections 3.1–3.4, respectively. A discussion of the results is presented in Section 3.5.

In the case of perpendicular shadow edge movement, every string is under uniform irradiance conditions. Thus, no mismatch losses occur in the MS configuration where every string is controlled individually and the mismatch losses of the SP and TCT configurations are equal and negligible. When a shadow edge moves parallel to the strings, every configuration behaves such as a single series-connected PV string. Thus, the mismatch losses of all the configurations are equal [11, 12].

3.1 Effect of SS

The relative mismatch losses of all the studied PV generators during a typical irradiance transition are presented as a function of the SS in Fig. 2 for apparent directions of movement of 0° and 30° and in Fig. 3 for apparent directions of movement of 60° and 90°. The relative mismatch losses increase with the increasing SS and with the increasing angle between the apparent direction of movement and direction perpendicular to the PV strings. The relative mismatch losses increase also with the increasing length of the strings, except in the case of perpendicular shadow edge movement. When a shadow edge moves perpendicular to the strings, every string is under uniform irradiance conditions and the relative mismatch losses of the SP and TCT configurations decrease with the decreasing number of the strings. Differences between the electrical configurations are minimal. Note that the mismatch losses are more than two orders of magnitude smaller for the perpendicular direction of movement than for the other directions.

The maximum instantaneous relative mismatch losses of all the studied PV generators are presented as a function of the SS in Fig. 4 while a typical shadow edge moves over the generator parallel to the strings. The maximum instantaneous mismatch losses increase with the increasing SS and with the increasing length of the strings. The maximum instantaneous mismatch losses are 49.3, 42.1 and 28.9% for string lengths of 28, 21 and 14 modules, respectively.

3.2 Effect of parameter b

The relative mismatch losses of all the studied PV generators during a typical irradiance transition are presented as a function of parameter b in Fig. 5 for apparent directions of movement of 0° and 30° and in Fig. 6 for apparent directions of movement of 60° and 90°. The mismatch losses decrease with increasing b which is understandable because the higher is b , the gentler is the irradiance transition, i.e. the smaller are the irradiance differences between adjacent modules. Again, the relative mismatch losses increase with the increasing angle between the apparent direction of movement and direction perpendicular to the strings and with the increasing length of the strings. In practice, there are no differences between the electrical configurations at values of b higher than 1 s. However, some differences exist at small values of b . A fold can be seen in the relative mismatch losses of the MS configuration at small values of b in Figs. 5b and 6a. This is in agreement with [11], where the relative mismatch losses of the MS configuration have been found to turn down as the length of the PV strings increases with respect to the length of the irradiance transition in the case of diagonal shadow edge movement across the PV array.

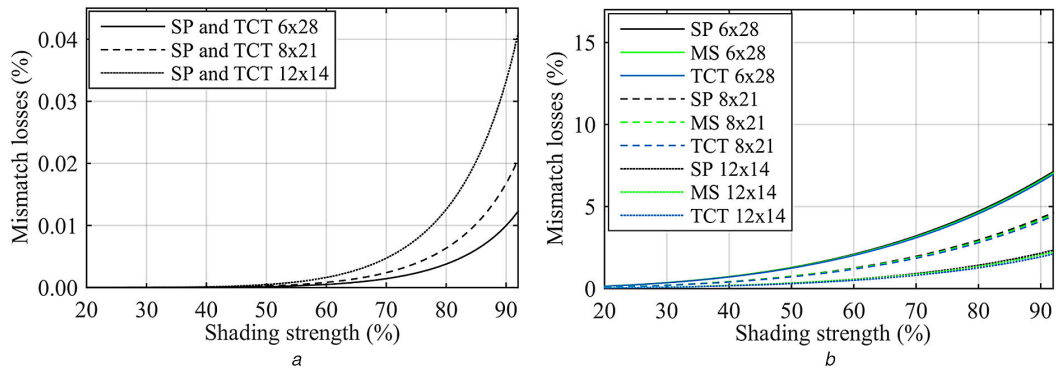


Fig. 2 Relative mismatch losses of the SP, MS and TCT configurations as a function of the SS during partial shading caused by the movement of a typical shadow edge over the PV generator

(a) Apparent movement direction of the shadow edge of 0°, (b) Apparent movement direction of the shadow edge of 30°

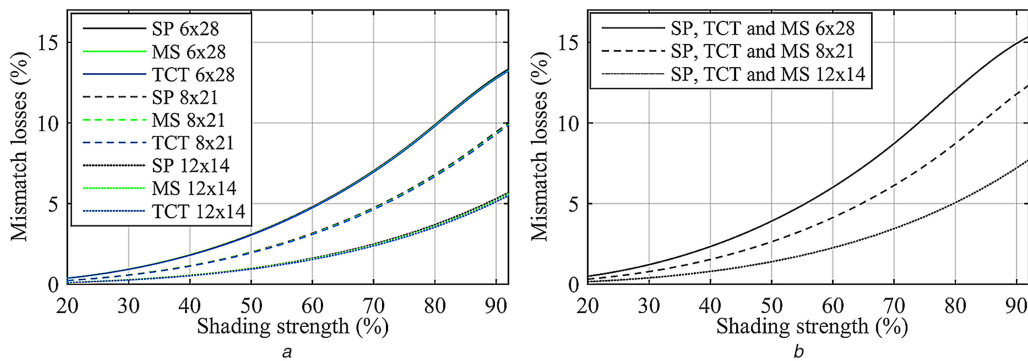


Fig. 3 Relative mismatch losses of the SP, MS and TCT configurations as a function of the SS during partial shading caused by the movement of a typical shadow edge over the PV generator

(a) Apparent movement direction of the shadow edge of 60°, (b) Apparent movement direction of the shadow edge of 90°

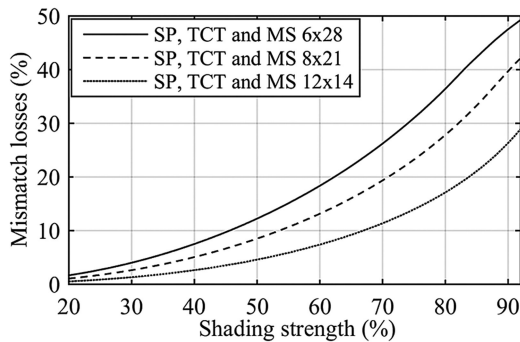


Fig. 4 Maximum instantaneous relative mismatch losses of the SP, MS and TCT configurations as a function of the SS during partial shading caused by the movement of a typical shadow edge over the PV generator parallel to the PV strings

The maximum instantaneous relative mismatch losses of all the studied PV generators are presented as a function of parameter b in Fig. 7 while a typical shadow edge moves over the generator parallel to the strings. The maximum instantaneous mismatch losses behave similarly than relative mismatch losses in Fig. 6b, except at very small values of b . At very small values, the maximum instantaneous relative mismatch losses decrease with decreasing b and with b of 0.1 s the maximum relative mismatch losses decrease with the increasing length of the strings. However, the differences are small. The maximum instantaneous mismatch losses are 34.5, 34.2 and 33.6% for string lengths of 28, 21 and 14 modules, respectively.

3.3 Effect of apparent speed

The relative mismatch losses of all the studied PV generators during a typical irradiance transition are presented as a function of the apparent speed of the shadow edge in Fig. 8 for apparent

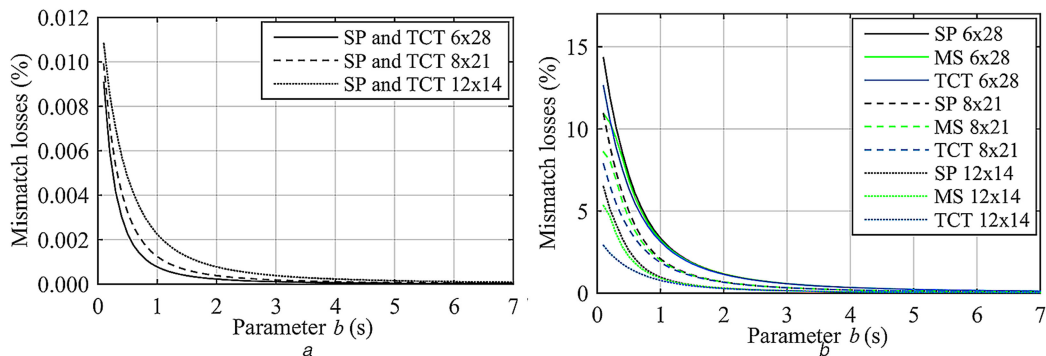


Fig. 5 Relative mismatch losses of the SP, MS and TCT configurations as a function of parameter b during partial shading caused by the movement of a typical shadow edge over the PV generator

(a) Apparent movement direction of the shadow edge of 0°, (b) Apparent movement direction of the shadow edge of 30°

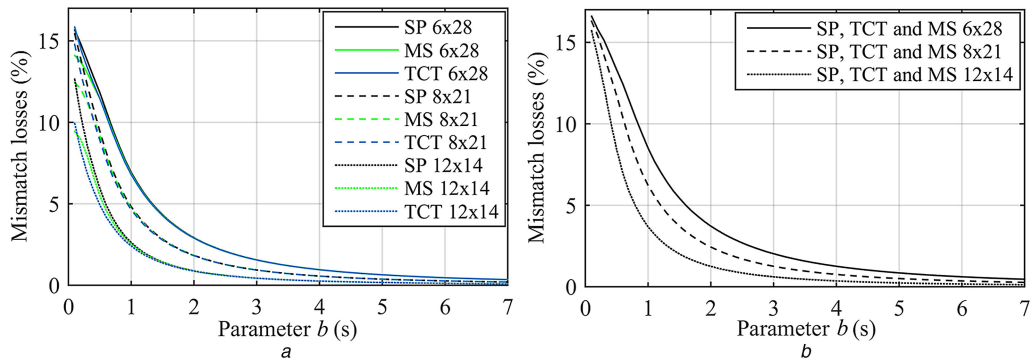


Fig. 6 Relative mismatch losses of the SP, MS and TCT configurations as a function of parameter b during partial shading caused by the movement of a typical shadow edge over the PV generator
 (a) Apparent movement direction of the shadow edge of 60° , (b) Apparent movement direction of the shadow edge of 90°

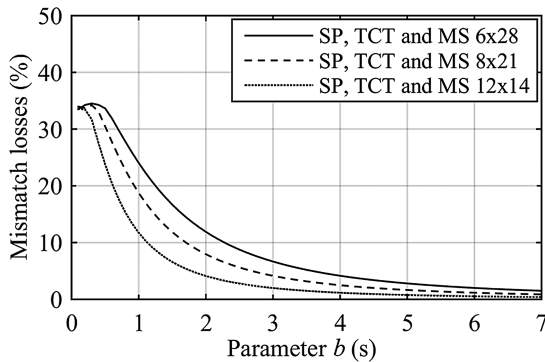


Fig. 7 Maximum instantaneous relative mismatch losses of the SP, MS and TCT configurations as a function of parameter b during partial shading caused by the movement of a typical shadow edge parallel to the PV strings

directions of movement of 0° and 30° and in Fig. 9 for apparent directions of movement of 60° and 90° . The behaviour of mismatch losses as a function of the apparent speed is qualitatively similar than as a function of b in Section 3.2, since both of these variables have an effect on the length of the transition. The relative mismatch losses decrease with the increasing speed and, again, increase with the increasing angle between the apparent direction of movement and direction perpendicular to the strings and with the increasing length of the strings. In practice, there are no differences between the electrical configurations, except at slow speeds.

The maximum instantaneous relative mismatch losses of all the studied PV generators are presented as a function of the apparent speed in Fig. 10 while a typical shadow edge moves over the generator parallel to the strings. The maximum instantaneous mismatch losses behave qualitatively similarly than in the case of parameter b (Fig. 7). They decrease with the increasing apparent speed, except at very slow speeds. The maximum instantaneous mismatch losses take place at low speeds and are almost the same

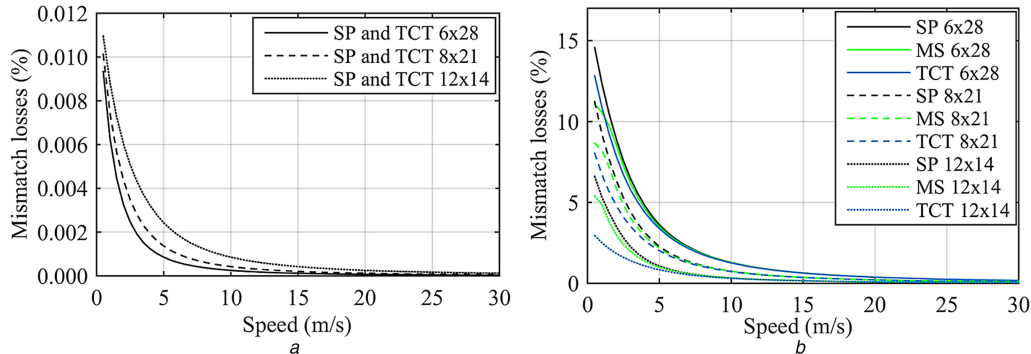


Fig. 8 Relative mismatch losses of the SP, MS and TCT configurations as a function of the apparent speed during partial shading caused by the movement of a typical shadow edge over the PV generator
 (a) Apparent movement direction of the shadow edge of 0° , (b) Apparent movement direction of the shadow edge of 30°

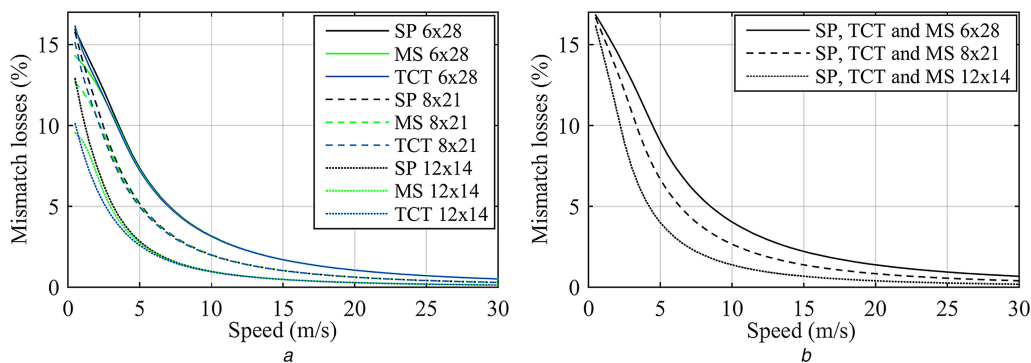


Fig. 9 Relative mismatch losses of the SP, MS and TCT configurations as a function of the apparent speed during partial shading caused by the movement of a typical shadow edge over the PV generator
 (a) Apparent movement direction of the shadow edge of 60° , (b) Apparent movement direction of the shadow edge of 90°

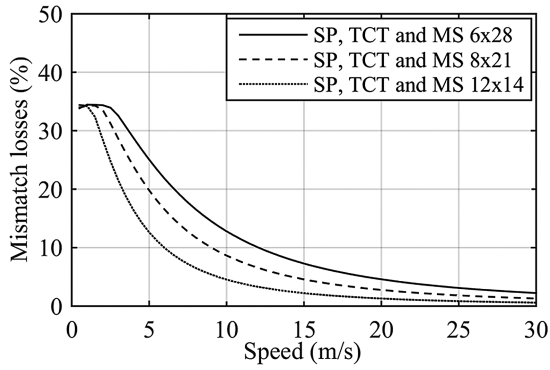


Fig. 10 Maximum instantaneous relative mismatch losses of the SP, MS and TCT configurations as a function of the apparent speed during partial shading caused by the movement of a typical shadow edge over the PV generator parallel to the PV strings

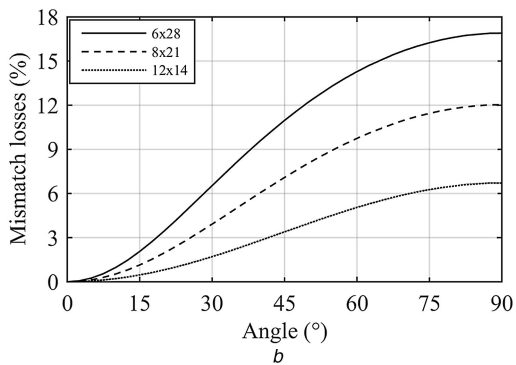
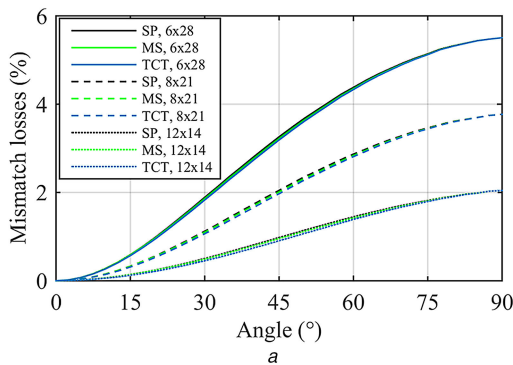


Fig. 11 Relative mismatch losses during partial shading caused by the movement of a typical shadow edge over the PV generator as a function of the apparent direction of movement of the shadow edge

(a) Relative mismatch losses of the SP, MS and TCT configurations during the irradiance transition, (b) Maximum instantaneous relative mismatch losses of the SP configuration

34.4, 34.4 and 34.2% for string lengths of 28, 21 and 14 modules, respectively.

3.4 Effect of direction of movement

The relative mismatch losses of all the studied PV generators during a typical irradiance transition are presented as a function of the apparent direction of movement of the shadow edge in Fig. 11a. The relative mismatch losses increase with the increasing angle between the apparent direction of movement of the shadow edge and direction perpendicular to the PV strings from almost zero to close to 6% for the longest PV module strings. This is plausible, since all the PV modules in a string are under the same irradiance when the shadow edge moves perpendicular to the strings and irradiance differences within the strings increase with the increasing angle. Again, there are only minor differences between the studied electrical PV array configurations, which means that the mismatch losses are almost independent of the electrical PV array configuration during irradiance transitions caused by moving clouds. The differences between the configurations are the biggest at angles around 45°. Furthermore, it is notable that the relative mismatch losses increase considerably with the increasing length of the strings being almost three times higher for the generators having strings of 28 PV modules than for the generators having strings of 14 modules.

The maximum instantaneous relative mismatch losses of the SP configuration during a typical irradiance transition are presented as a function of the apparent direction of movement of the shadow edge in Fig. 11b. The mismatch losses are, in practice, the same for the other two electrical PV array configurations. The maximum instantaneous mismatch losses are over three times higher than the mismatch losses in Fig. 11a, but otherwise behave similarly. The maximum instantaneous mismatch losses are 16.9, 12.0 and 6.7% for string lengths of 28, 21 and 14 modules, respectively.

3.5 Discussion

Since the length of an irradiance transition is calculated as the product of the duration and apparent speed of the transition, both the apparent speed and parameter b have an effect on the length of the transition. Thus, the mismatch losses behave similarly as a function of these variables and the same phenomena can be observed by studying the mismatch losses as functions of these variables.

The relative mismatch losses are the largest in the case of parallel shadow edge movement with respect to the PV strings in line with the findings of [11, 12]. It has been found in [12] that in the case of parallel shadow edge movement the mismatch losses reach the maximum values when the length of the PV strings is roughly twice the length of the irradiance transition. When a typical apparent irradiance transition speed is assumed, the corresponding values of b for the studied PV arrays are 0.34, 0.26 and 0.17 s for string lengths of 28, 21 and 14 modules, respectively. The phenomenon observed in [12] cannot be

confirmed directly based on Fig. 6b. However, the maximum instantaneous relative mismatch losses can be observed to achieve the highest values around these values of b in Fig. 7. The same phenomenon can be observed also from the maximum instantaneous relative mismatch losses as a function of the apparent speed in Fig. 10. In [12], irradiance transitions were assumed to be linear and were simulated by only five, seven and nine different irradiance values which simplified the simulations and effected to the results compared with this paper. Moreover, in [12], irradiance transitions were very large (SS of 90%) and steep. As a conclusion, it can be stated that the results obtained in this paper are in general agreement with [12], but mismatch losses caused by partial shading of the PV generators due to the movement of cloud shadow edges are not as severe as anticipated earlier.

Only minor differences were observed between the mismatch losses of the studied electrical PV array configurations. Reason for this is that the length of a typical irradiance transition region [19] is much longer than the diameters of PV arrays. Only the steepest and fastest shadow edges bring about some differences on the operation of different electrical PV array configurations. This is a notable result indicating that the studies related to different electrical PV array configurations are useless on the point of view of real applications. Moreover, it has been found in [23] that the PV array power fluctuations caused by moving clouds are practically the same for the SP, TCT and MS configurations. The other notable finding of real practical importance is that the mismatch losses due to irradiance transitions caused by moving clouds increase more than linearly with the increasing length of the PV module strings, except in the case of perpendicular shadow edge movement. However, in the case of perpendicular shadow edge movement, the mismatch losses are negligible. The conclusion is that PV module strings should not be installed in straight rows. Instead, the diameter of the PV module string area should be minimised to minimise the mismatch losses in accordance with earlier findings [10]. Third notable finding is that the apparent direction of movement of shadow edges has a notable effect on the mismatch

losses. On the basis of the results, PV arrays should be placed so that the dominant apparent direction of movement of shadow edges is perpendicular to the PV strings as presented earlier in [11, 12].

4 Conclusion

In this paper, the effects of irradiance transition characteristics on the mismatch losses of different electrical PV array configurations were studied. This study was based on theoretical simulations conducted by using a mathematical model of irradiance transitions and an experimentally verified MATLAB Simulink model of a PV module based on the well-known one-diode model of a PV cell. Irradiance transitions were fully characterised by four variables: SS, duration related parameter b , apparent speed and apparent direction of movement. Since the variables do not correlate with each other, their effects could be studied independently. The effects of the variables were studied by changing the value of the studied variable within experimentally observed limits while keeping the values of the other variables fixed at typical observed shadow edge parameter values. The studied electrical PV array configurations were SP, TCT and MS. Furthermore, three different physical shapes of the configurations, i.e. lengths of PV strings, were studied.

The mismatch losses were observed to increase considerably with the increasing angle between the apparent direction of movement of cloud shadow edges and direction perpendicular to the PV strings. Thus, PV arrays should be placed so that the dominant apparent direction of movement of shadow edges is perpendicular to the PV strings. The mismatch losses increased also with increasing SS and decreased with the increasing value of parameter b and apparent speed of transitions, except at very small values. The largest observed instantaneous relative mismatch losses were almost 50%.

Perhaps the most important finding of this paper is that the mismatch losses during irradiance transitions caused by moving clouds are practically the same for the studied electrical PV array configurations. Reason for this is that the length of a typical irradiance transition region is much longer than the diameters of PV arrays. Only the steepest and fastest shadow edges bring about some differences on the operation of different electrical PV array configurations. This indicates that the studies related to different electrical PV array configurations of SP, MS, TCT etc. are useless on the point of view of real applications. From the mismatch losses point of view, one can just use the simplest electrical configuration for PV arrays. The other important finding is that the mismatch losses due to irradiance transition caused by moving clouds increase more than linearly with the increasing length of the PV module strings. The conclusion is that the diameter of the PV module string area should be minimised to decrease the mismatch losses and thus improve the efficiency of the PV system.

5 References

- [1] Lappalainen, K., Valkealahti, S.: 'Analysis of shading periods caused by moving clouds', *Sol. Energy*, 2016, **135**, pp. 188–196
- [2] Patel, H., Agarwal, V.: 'MATLAB-based modeling to study the effects of partial shading on PV array characteristics', *IEEE Trans. Energy Convers.*, 2008, **24**, (1), pp. 302–310
- [3] Wang, Y.-J., Hsu, P.-C.: 'An investigation on partial shading of PV modules with different connection configurations of PV cells', *Energy*, 2011, **36**, (5), pp. 3069–3078
- [4] Bidram, A., Davoudi, A., Balog, R.S.: 'Control and circuit techniques to mitigate partial shading effects in photovoltaic arrays', *IEEE J. Photovolt.*, 2012, **2**, (4), pp. 532–546
- [5] Mäki, A., Valkealahti, S., Leppäaho, J.: 'Operation of series-connected silicon-based photovoltaic modules under partial shading conditions', *Prog. Photovolt. Res. Appl.*, 2012, **20**, (3), pp. 298–309
- [6] Villa, L.F.L., Picault, D., Raison, B., *et al.*: 'Maximizing the power output of partially shaded photovoltaic plants through optimization of the interconnections among its modules', *IEEE J. Photovolt.*, 2012, **2**, (2), pp. 154–163
- [7] Belhachat, F., Larbes, C.: 'Modeling, analysis and comparison of solar photovoltaic array configurations under partial shading conditions', *Sol. Energy*, 2015, **120**, pp. 399–418
- [8] Psarros, G.N., Batzelis, E.I., Papanthassiou, S.A.: 'Partial shading analysis of multistring PV arrays and derivation of simplified MPP expressions', *IEEE Trans. Sustain. Energy*, 2015, **6**, (2), pp. 499–508
- [9] Shams El-Dein, M.Z., Kazerani, M., Salama, M.M.A.: 'Optimal photovoltaic array reconfiguration to reduce partial shading losses', *IEEE Trans. Sustain. Energy*, 2013, **4**, (1), pp. 145–153
- [10] Mäki, A., Valkealahti, S.: 'Mismatch losses in photovoltaic power generators due to partial shading caused by moving clouds'. Proc. 27th European Photovoltaic Solar Energy Conf., Frankfurt, Germany, September 2012, pp. 3911–3915
- [11] Lappalainen, K., Mäki, A., Valkealahti, S.: 'Effects of the size of PV arrays on mismatch losses under partial shading conditions caused by moving clouds'. Proc. 28th European Photovoltaic Solar Energy Conf., Paris, France, September 2013, pp. 4071–4076
- [12] Lappalainen, K., Mäki, A., Valkealahti, S.: 'Effects of the sharpness of shadows on the mismatch losses of PV generators under partial shading conditions caused by moving clouds'. Proc. 28th European Photovoltaic Solar Energy Conf., Paris, France, September 2013, pp. 4081–4086
- [13] Sánchez Reinoso, C.R., Milone, D.H., Buitgaro, R.H.: 'Simulation of photovoltaic centrals with dynamic shading', *Appl. Energy*, 2013, **103**, pp. 278–289
- [14] Mäki, A., Valkealahti, S.: 'Differentiation of multiple maximum power points of partially shaded photovoltaic power generators', *Renew. Energy*, 2014, **71**, pp. 89–99
- [15] Tomson, T.: 'Fast dynamic processes of solar radiation', *Sol. Energy*, 2010, **84**, pp. 318–323
- [16] Tomson, T., Hansen, M.: 'Dynamic properties of clouds *Cumulus humilis* and *Cumulus fractus* extracted by solar radiation measurements', *Theor. Appl. Climatol.*, 2011, **106**, (1), pp. 171–177
- [17] Tomson, T.: 'Transient processes of solar radiation', *Theor. Appl. Climatol.*, 2013, **112**, (3), pp. 403–408
- [18] Lappalainen, K., Valkealahti, S.: 'Recognition and modelling of irradiance transitions caused by moving clouds', *Sol. Energy*, 2015, **112**, pp. 55–67
- [19] Lappalainen, K., Valkealahti, S.: 'Apparent velocity of shadow edges caused by moving clouds', *Sol. Energy*, 2016, **138**, pp. 47–52
- [20] Lave, M., Reno, M.J., Broderick, R.J.: 'Characterizing local high-frequency solar variability and its impact to distribution studies', *Sol. Energy*, 2015, **118**, pp. 327–337
- [21] Perez, R., Kivalov, S., Schlemmer, J., *et al.*: 'Parameterization of site-specific short-term irradiance variability', *Sol. Energy*, 2011, **85**, pp. 1343–1353
- [22] Lappalainen, K., Valkealahti, S.: 'Mathematical parametrisation of irradiance transitions caused by moving clouds for PV system analysis'. Proc. 32nd European Photovoltaic Solar Energy Conf., Munich, Germany, June 2016, pp. 1485–1489
- [23] Lappalainen, K., Valkealahti, S.: 'Effects of irradiance transitions on the output power fluctuations of different PV array configurations'. Proc. IEEE Innovative Smart Grid Technologies – Asia Conf., Melbourne, Australia, November–December 2016, pp. 705–711
- [24] Villalva, M.G., Gazoli, J.R., Filho, E.R.: 'Comprehensive approach to modeling and simulation of photovoltaic arrays', *IEEE Trans. Power Electron.*, 2009, **24**, (5), pp. 1198–1208
- [25] Wenham, S.R., Green, M.A., Watt, M.E., *et al.*: '*Applied photovoltaics*' (Earthscan, London, UK, 2007, 2nd edn.)
- [26] Torres Lobera, D., Mäki, A., Huusari, J., *et al.*: 'Operation of TUT solar PV power station research plant under partial shading caused by snow and buildings', *Int. J. Photoenergy*, 2013, **2013**, pp. 1–13